Table 2 Comparison of long-term and short-term survivors

Factor	Category	*n*	Survivors ($N = 229$)		*P*
			<5 yr ($n = 189$)	≥5 yr ($n = 40$)	
Ca19-9	≤206	115	88	27	0.023
(median 206 IU/dl)	>206	114	101	13	
Location	Head/neck	157	132	25	0.364
	Body/tail	72	57	15	
Size	≤35	118	90	28	0.014
(median 36 mm: 8–110)	>35	111	99	12	
Lymph node involvement	Absent	38	22	16	0.000
	Present	191	167	24	
Serosal invasion	Absent	179	144	35	0.058
	Present	50	45	5	
Retroperitoneal invasion	0/1	106	78	28	0.001
	2/3	123	111	12	
Portal vein invasion	Negative	120	94	26	0.085
	Positive	109	95	14	
Plexus invasion	Absent	143	116	27	0.491
	Present	85	72	13	
Differentiation	Well	68	53	15	0.234
	Mod/poor	161	136	25	
Lymphatic invasion	0/1	102	73	29	0.000
	2/3	127	116	11	
Venous invasion	0/1	97	73	24	0.002
	2/3	132	116	16	
Intrapancreatic nerve invasion	0/1	97	73	24	0.014
	2/3	132	116	16	
Stage (UICC 6th) [IA ($n = 3$), 2A ($n = 32$), 2B ($n = 143$)]	<III	178	141	37	0.013
Stage (UICC 6th) [III ($n = 16$), IV ($n = 35$)]	≥III	51	48	3	
Surgical margin status	Negative	154	123	31	0.142
	Positive	75	66	9	
Intraoperative radiotherapy	Yes	159	135	24	0.154
	No	70	54	16	
Adjuvant chemotherapy	Yes	59	46	13	0.284
	No	170	143	27	

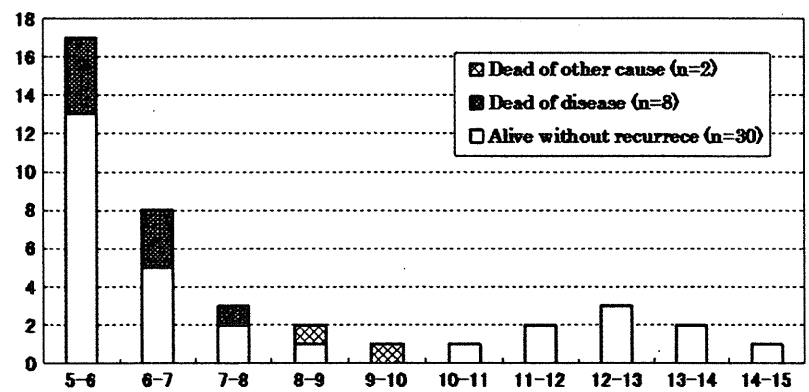

Fig. 2 Status of each 5-year survivor in the following years and the cause of death in those who did not survive (*x*-axis: years after 5 years survival; and *y*-axis: number of patients)

Table 3 Characteristic features of the 5-year survivors with disease recurrence

No./age (yr)/sex	CA19-9 (U/ml)[a]	Site	Size (cm)	Operation	Stage	Curability	Initial recurrence site	Treatment for recurrence	Recurrence after operation (yr)	Outcome (yr)
1/47/F	214	Ph	3.8	PD, PV	2B	R0	Unknown[c]	None	4.4	6.0 D
2/70/M	399	Ph	2.3	PD	2A	R0	Lung	None	5.3	5.7 D
3/62/M	3000	Ph	4.8	PD, PV	2B	R1	Bone	Radiation	3.4	6.2 D
4/60/F	156	Pb	5.5	DP	2B	R1	Local	Resection, chemotherapy	1.5	6.6 D
5/80/M	1658	Ph	2.2	PD	2B	R1	Bone	None	4.1	7.3 D
6/51/F	15	Ph	1.5	PD	2B	R0	Lung	None	3.9	5.1 D
7/63/F	792	Ph	4.0	PD	2B	R0	Bone	Radiation	3.5	12.6 A
8/56/M	526	T	11.0	TP, PV	2B[b]	R0	Lymph nodes	Chemotherapy	1.0	5.0 D
9/63/F	48	Pb	2.8	DP	2B	R1	Pleural cavity	Chemotherapy	3.5	5.4 D
10/27/F	211	Ph	5.0	PD, PV, AR	III	R1	Local	Radiation, chemotherapy	0.4	5.2 A

PD pancreaticoduodenectomy, *PV* portal vein resection, *AR* common hepatic artery resection and reconstruction, *DP* distal pancreatectomy, *LN* lymph nodes, *A* alive, *D* death

[a] CA19-9 at surgery, stage was defined as UICC 6th

[b] Positive washing cytology

[c] CA19-9 was remarkably elevated but recurrence site could not be evaluated

Table 4 Factors influencing an additional 5-year survival in the 40 patients surviving more than 5 years after a macroscopic curative pancreatectomy

Factor	Category	*n*	10-yr survival (%)	Mean survival term (yr)	*P*
Lymph node involvement	Absent	16	90	12.9 ± 0.8	0.1021
	Present	24	61	11.2 ± 1.0	
Retroperitoneal invasion	0/1	28	74	12.3 ± 0.8	0.4859
	2/3	12	69	10.2 ± 1.4	
Lymphatic invasion	0/1	29	78	12.6 ± 0.7	0.1464
	2/3	11	45	9.5 ± 1.8	
Intrapancreatic nerve invasion	0/1	24	83	11.5 ± 0.6	0.0499
	2/3	16	49	10.1 ± 1.4	
Surgical margin status	Negative	31	79	13.0 ± 0.7	0.0893
	Positive	9	50	8.9 ± 1.1	

difficult to predict 5-year survival based on common clinical parameters alone.

The present study found that limited cancer extension with negative lymph node metastases significantly contributes to the chance of surviving more than 5 years, but a macroscopic curative pancreatectomy should be recommended for patients with a more advanced stage because of the possibility of 5-year survival. A surgical cure could not always be expected, even in patients surviving more than 5 years, especially those with a higher incidence of intrapancreatic neural invasion or a positive surgical margin status.

Acknowledgments This study was supported by a Grant-in-Aid for cancer research from the Ministry of Health, Labour and Welfare of Japan.

The authors have no direct or indirect commercial and financial incentive associated with publishing the article.

References

1. Conlon KC, Klimstra DS, Brennan MF (1996) Long-term survival after curative resection for pancreatic ductal adenocarcinoma: clinicopathologic analysis of 5-year survivors. Ann Surg 223:273–279
2. Matsuno S, Egawa S, Fukuyama S et al (2004) Pancreatic Cancer Registry in Japan: 20 years of experience. Pancreas 28:219–230
3. Sohn TA, Yeo CJ, Cameron JL et al (2000) Resected adenocarcinoma of the pancreas 616 patients: results, outcomes, and prognostic indicators. J Gastrointest Surg 4:567–579
4. Oettle H, Post S, Neuhaus P et al (2007) Adjuvant chemotherapy with gemcitabine vs. observation in patients undergoing

curative-intent resection of pancreatic cancer. A randomized control trial. JAMA 297:267–277
5. Cleary SP, Gryfe R, Guindi W et al (2004) Prognostic factors in resected pancreatic adenocarcinoma: analysis of 5-year survivors. J Am Coll Surg 198:722–731
6. Riall TS, Cameron JL, Lillemoe KD et al (2006) Resected periampullary adenocarcinoma: 5-year survivors and their 6- to-10-year follow-up. Surgery 140:764–772
7. Han SS, Jang JY, Kim SW, Kim WH, Lee KU, Park YH (2006) Analysis of long-term survivors after surgical resection for pancreatic cancer. Pancreas 32:271–275
8. Schnelldorfer T, Ware AL, Sarr MG et al (2008) Long-term survival after pancreatoduodenectomy for pancreatic adenocarcinoma. Is cure possible? Ann Surg 247:456–462
9. Adham M, Jaeeck D, Borgne JL et al (2008) Long-term survival (5–20 years) after pancreatectomy for pancreatic ductal adenocarcinoma. A series of 30 patients collected from 3 institutions. Pancreas 37:352–357
10. Ferrone CR, Brennan MF, Gonen M et al (2008) Pancreatic adenocarcinoma: the actual 5-year survivors. J Gastrointest Surg 12:701–706
11. Katz MHG, Wang H, Fleming JB et al (2009) Long-term survival after multidisciplinary management of resected pancreatic adenocarcinoma. Ann Surg Oncol 16:836–847
12. Japan Pancreas Society (2003) Classification of pancreatic carcinoma, 2nd English edn. Kanehara, Tokyo
13. Sobin LH, Wittekind Ch (eds) (2002) International Union against Cancer. TNM classification of malignant tumors, 6th edn. Wiley, New York
14. Shimada K, Kosuge T, Yamamoto Y, Yamasaki S, Sakamoto M (2004) Successful outcome after resection of pancreatic cancer with a solitary hepatic metastasis. Hepatogastroenterology 51:603–605
15. Ishikawa O, Ohhigashi H, Sasaki Y et al (1988) Practical usefulness of lymphatic and connective tissue clearance for the carcinoma of the pancreas head. Ann Surg 208:215–220
16. Löttges J, Vogel I, Menke M, Henne-Bruns D, Kremer B, Klöppel G (1998) The retroperitoneal resection margin and vessel involvement are important factors determining survival after pancreaticoduodenectomy for ductal adenocarcinoma of the head of the pancreas. Virchows Arch 433:237–242
17. Helm J, Centeno BA, Coppola D et al (2009) Histologic characteristics enhance predictive value of American Joint Committee on Cancer Staging in resectable pancreas cancer. Cancer 115:4080–4089
18. Ozaki H, Hiraoka T, Mizumoto R et al (1999) The prognostic significance of lymph node metastases and intrapancreatic perineural invasion in pancreatic cancer after curative resection. Surg Today 29:16–22
19. Ceyhan GO, Bergmann F, Kadihasanoglu M et al (2009) Pancreatic neuropathy and neuropathic pain: a comprehensive pathomorphological study of 546 cases. Gastroenterology 136:177–186
20. Magnin V, Viret F, Moutardier V et al (2004) Complete pathologic responses to preoperative chemoradiation in two patients with adenocarcinoma of the pancreas. Pancreas 28:103–104
21. Le Scodan R, Mornex F, Partensky C et al (2008) Histopathological response to preoperative chemoradiation for resectable pancreatic adenocarcinoma: the French Phase II FFCD 9704-SFRO Trial. Am J Clin Oncol 31:545–552
22. Egawa S, Takeda K, Fukuyama S, Motoi F, Sunamura M, Matsuno S (2004) Clinicopathological aspect of small pancreatic cancer. Pancreas 28:235–240
23. Gleisner AL, Assumpcao L, Cameron JL et al (2007) Is resection of periampullary or pancreatic adenocarcinoma with synchronous hepatic metastasis justified? Cancer 110:2484–2492
24. Stitzenberg KB, Watson JC, Roberts A et al (2008) Survival after pancreatectomy with major arterial resection and reconstruction. Ann Surg Oncol 15:1399–1406

Published OnlineFirst May 25, 2010; DOI:10.1158/0008-5472.CAN-10-0220

AACR

Cancer Research

CUB Domain–Containing Protein 1, a Prognostic Factor for Human Pancreatic Cancers, Promotes Cell Migration and Extracellular Matrix Degradation

Yuri Miyazawa, Takamasa Uekita, Nobuyoshi Hiraoka, et al.

Cancer Res 2010;70:5136-5146. Published OnlineFirst May 25, 2010.

Published OnlineFirst May 25, 2010; DOI:10.1158/0008-5472.CAN-10-0220

Tumor and Stem Cell Biology

Cancer Research

CUB Domain–Containing Protein 1, a Prognostic Factor for Human Pancreatic Cancers, Promotes Cell Migration and Extracellular Matrix Degradation

Yuri Miyazawa[1,4], Takamasa Uekita[1], Nobuyoshi Hiraoka[2], Satoko Fujii[1], Tomoo Kosuge[3], Yae Kanai[2], Yoshihisa Nojima[4], and Ryuichi Sakai[1]

Abstract

CUB domain–containing protein 1 (CDCP1) is a membrane protein that is highly expressed in several solid cancers. We reported previously that CDCP1 regulates anoikis resistance as well as cancer cell migration and invasion, although the underlying mechanisms have not been elucidated. In this study, we found that expression of CDCP1 in pancreatic cancer tissue was significantly correlated with overall survival and that CDCP1 expression in pancreatic cancer cell lines was relatively high among solid tumor cell lines. Reduction of CDCP1 expression in these cells suppressed extracellular matrix (ECM) degradation by inhibiting matrix metalloproteinase-9 secretion. Using the Y734F mutant of CDCP1, which lacks the tyrosine phosphorylation site, we showed that CDCP1 regulates cell migration, invasion, and ECM degradation in a tyrosine phosphorylation–dependent manner and that these CDCP1-associated characteristics were inhibited by blocking the association of CDCP1 and protein kinase Cδ (PKCδ). CDCP1 modulates the enzymatic activity of PKCδ through the tyrosine phosphorylation of PKCδ by recruiting PKCδ to Src family kinases. Cortactin, which was detected as a CDCP1-dependent binding partner of PKCδ, played a significant role in migration and invasion but not in ECM degradation of pancreatic cells. These results suggest that CDCP1 expression might play a crucial role in poor outcome of pancreatic cancer through promotion of invasion and metastasis and that molecules blocking the expression, phosphorylation, or the PKCδ-binding site of CDCP1 are potential therapeutic candidates. *Cancer Res; 70(12); 5136–46. ©2010 AACR.*

Introduction

CUB domain–containing protein 1 (CDCP1) is a type I transmembrane protein with several tyrosine residues that can be phosphorylated by Src family kinases (SFK; refs. 1–5). CDCP1 was first identified as the product of a gene preferentially expressed in colon cancer cells compared with normal tissue (1). We recently reported that tyrosine-phosphorylated CDCP1 in lung cancer cells plays a novel role in acquiring resistance to anoikis, a type of cell death caused by detachment from extracellular matrix (ECM). CDCP1 was reported to directly bind to protein kinase Cδ (PKCδ) at a unique C2 domain—a novel phosphotyrosine-binding domain—in a phosphorylation-dependent manner (4). The biological meaning of interaction with PKCδ had not been revealed until we recently discovered that tyrosine-phosphorylated CDCP1 regulates the anoikis resistance of lung cancer cells by acting as a physical link between SFKs and PKCδ, which is a putative cell death–associated molecule (5). Using scirrhous gastric cancer cells, we further reported that phosphorylation of CDCP1 promotes cell migration and invasion *in vitro* and peritoneal dissemination *in vivo* in mice (6). Recent studies of lung adenocarcinoma and renal cell carcinoma have shown that CDCP1 expression has important associations with disease progression (7, 8). Despite accumulating evidence showing the significant involvement of CDCP1 in tumor progression, metastasis, and invasion, the role of the CDCP1 signaling pathway during these biological procedures is not yet well understood.

Pancreatic cancer is one of the most malignant tumors, with poor prognosis due to its aggressive behavior and high metastatic potential. Moreover, pancreatic cancer is sometimes accompanied with specific types of invasion, such as perineural invasion, which can cause severe pain and discomfort. Appropriate treatment that inhibits invasion and metastasis of pancreatic cancers is urgently required to improve both the survival and quality of life of patients.

In this study, we found that CDCP1 is expressed in primary pancreatic tumors as well as in sites of invasion and metastasis of pancreatic cancer. We analyzed the expression levels

Authors' Affiliations: [1]Growth Factor Division and [2]Pathology Division, National Cancer Center Research Institute and [3]Division of Hepato-Biliary and Pancreatic Surgery, National Cancer Center Hospital, Tokyo, Japan and [4]Department of Medicine and Clinical Science, Gunma University Graduate School of Medicine, Gunma, Japan

Note: Supplementary data for this article are available at Cancer Research Online (http://cancerres.aacrjournals.org/).

Corresponding Author: Ryuichi Sakai, National Cancer Center Research Institute, 5-1-1 Tsukiji, Chuo-ku, Tokyo 104-0045, Japan. Phone: 81-3-3547-5247; Fax: 81-3-3542-8170; E-mail: rsakai@ncc.go.jp.

doi: 10.1158/0008-5472.CAN-10-0220

Published OnlineFirst May 25, 2010; DOI:10.1158/0008-5472.CAN-10-0220

of CDCP1 protein in human pancreatic cancer tissues by using immunohistochemistry and discovered that high CDCP1 expression is correlated with poor prognosis. Tyrosine phosphorylation of CDCP1 was also shown to be essential for ECM degradation in pancreatic cancer through the formation of the CDCP1-PKCδ complex and enzymatic activation of PKCδ in highly invasive pancreatic cancer cell lines. Our results suggest that CDCP1 is a promising therapeutic target that modulates metastasis and invasion of several cancer types.

Materials and Methods

Cell culture and transfection

Pancreatic (Suit4, Capan1, PANC1, BxPC3, and CFPAC1) and gastric (HSC44As3 and HSC59) cancer cell lines were cultured in RPMI 1640 with 10% fetal bovine serum (FBS) at 37°C with 5% CO_2. The fibrosarcoma cell line HT1080 was cultured in DMEM with 10% FBS. For transfection, cells were seeded on a plate at 2.0×10^6 per 10-cm dish, and transfection was performed after 24 hours. Expression plasmids were transfected with Lipofectamine 2000 according to the manufacturer's instructions (Invitrogen). Transfected cells were selected in the presence of G418 at the concentration of 1,200 μg/mL (BxPC3) or 900 μg/mL (Capan1).

Short interfering RNA treatment

Two sets of short interfering RNAs (siRNA) of CDCP1 were synthesized as described elsewhere (5). Two sets of siRNAs of PKCδ or cortactin were synthesized as follows: PKCδ siRNA-1, 5′-GGUGCAGAAGAAGCCGACCAUGUAU-3′ (sense) and 5′-AUACAUGGUCGGCUUCUUCUGCACC-3′ (antisense); PKCδ siRNA-2, 5′-CCAAGGUGUUGAUGGUCGGUUCAGUA-3′ (sense) and 5′-UACUGAACCGACCAUCAACACCUUGG-3′ (antisense); cortactin siRNA-1, 5′-CCCAGAAAGACUAUGUGAAAGGGUU-3′ (sense) and 5′-AACCCUUUCACAUAGUCUUUCUGGG-3′ (antisense); cortactin siRNA-2, 5′-GGAGAAGCACGAGUCACAGAGAGAU-3′ (sense) and 5′-AUCUCUCUGUGACUCGUGCUUCUCC-3′ (antisense). The control siRNA was Stealth RNAi Negative Control Medium GC Duplex. All siRNAs were obtained from Invitrogen. siRNAs (40 pmol) were incorporated into cells using Lipofectamine 2000 according to the manufacturer's instructions. Cells were used for further experiments at 72 hours after siRNA treatment.

Plasmids, antibodies, and reagents

Plasmids of human CDCP1 and of CDCP1 Y734F (Tyr^{734} to Phe) with FLAG tag have already been described (5). CDCP1 rescue mutant, which introduced silent mutations not to be suppressed by CDCP1 siRNA, with COOH terminus FLAG tag was generated by PCR using KOD-Plus-Mutagenesis kit (Toyobo Co. Ltd.). A cDNA fragment of the C2 domain of human PKCδ with hemagglutinin (HA) tag has already been described (5). The antibodies against PKCδ (C-20; 1:2,500), HA (Y-11; 1:2,500), and actin (I-19; 1:200) were purchased from Santa Cruz Biotechnology. The phospho-PKCδ (Tyr^{311}; 1:500) and phospho-PKCδ (Thr^{505}; 1:500) antibodies were from Cell Signaling. The FLAG M2 (1:5,000) and α-tubulin (1:10,000) antibodies were from Sigma. Polyclonal antibody against CDCP1 (1:500) and tyrosine-phosphorylated CDCP1 (Tyr^{734}; 1:1,000) was prepared as described previously (5). The monoclonal antibodies that recognize cortactin (clone 4F11; 1:5,000), matrix metalloproteinase-9 (MMP-9; 1:500), and phosphotyrosine (4G10; 1:2,500) were purchased from Millipore.

Western blotting and immunoprecipitation

Western blotting and immunoprecipitation were performed as described previously (5). Protein concentration was measured by bicinchoninic acid protein assay kit (Pierce). Supernatant was concentrated by 10% trichloroacetic acid precipitation, and then samples were washed twice with diethyl ether. Polyvinylidene difluoride membrane (Immobilon-P, Millipore) was used for the transfer membrane, and Blocking One (Nakarai Tesque) was used for the blocking of the membrane. For immunoprecipitation, 1,000 μg protein was mixed with 2 μg of each antibody, and then samples were rotated with protein G–Sepharose beads (GE Healthcare).

Cell migration and Matrigel invasion assay

Migration and invasion assay were performed using modified Transwell chambers with a polycarbonate nucleopore membrane (BD Falcon) as described previously (9). Cells treated with each siRNA were detached with trypsin-EDTA. Then, the cells in 100 μL of RPMI 1640 with 10% FBS were seeded onto the upper part of each chamber. After incubation for 6 hours for migration, and 18 hours (BxPC3) or 30 hours (Capan1) for invasion, the cells on the membrane were fixed. The totals of migrated or invaded cells were determined by counting the cells on the lower side of the membranes from two wells (two fields per membrane) at a magnification of ×100, and the extent of migration or invasion was expressed as the average ratio (number of cells transfected with siRNA per field/average number of cells transfected with control siRNA per field). The results were from three independent experiments.

ECM degradation assays

The 12-mm-round cover glasses were coated with fluorescein-conjugated type I collagen from bovine skin (Invitrogen) diluted at 1 μg/μL in PBS for 5 minutes at room temperature, and the cover glasses were dried out for 10 minutes at room temperature. The collagen-coated glasses were then fixed with 0.5% glutaraldehyde solution on ice for 10 minutes and at room temperature for 30 minutes. After washing six times with PBS, the glasses facing upward were transferred to each well of a 24-well plate containing 70% ethanol and incubated for 15 minutes. After two washes with PBS, 2×10^4 cells were plated onto the coated glass in RPMI 1640 containing 10% FBS. After 18 hours (BxPC3) or 30 hours (Capan1) of culture, cells were fixed and stained with Alexa phalloidin (1:100; Invitrogen) in PBS. The staining was visualized using a Radiance 2100 confocal microscopic system (Bio-Rad). The cells degrading collagen were determined to

Published OnlineFirst May 25, 2010; DOI:10.1158/0008-5472.CAN-10-0220

overlap the degradation area. Data in 20 fields at a magnification of ×800 were used to calculate the cells degrading collagen per total cells. The results were from three independent experiments.

Gelatin zymography

Gelatin zymography was conducted with a polyacrylamide gel containing gelatin (0.8 mg/mL) as described previously (10). The SDS-polyacrylamide gel was incubated for 24 hours in the incubation buffer with or without 2.7 nmol/L MMP inhibitor II (MMP-1, MMP-3, MMP-7, and MMP-9 inhibitor; Calbiochem) or DMSO at 37°C. Enzyme activity was visualized as negative staining with Coomassie brilliant blue.

Immunocytochemical staining

Immunocytochemical staining was performed as previously described (11). The cover glasses were coated by FBS for 1 hour before seeding the cells. For transfection, 5.0×10^4 cells were seeded on a glass and then fixed and stained. The staining was visualized using a confocal microscopic system (Bio-Rad).

Patients and tissue samples

Pancreatic tumor specimens were obtained from 158 patients who underwent surgery at the National Cancer Center Hospital (1990–2005; clinicopathologic findings from these 158 patients are summarized in Supplementary Table S1). The follow-up period for survivors ranged from 0.067 to 172.833 months (median, 14.433 mo). Tumors were classified according to the International Union Against Cancer tumor-node-metastasis classification (12), the classification of pancreatic carcinoma of the Japan Pancreas Society (13), and the WHO classification (14). The study was approved by the ethical review board of the National Cancer Center. Informed consent was obtained from each patient.

Immunohistochemistry

Immunohistochemical staining was performed on the formalin-fixed, paraffin-embedded slides using the avidin-biotin complex method, as described previously (15). A specific antibody against CDCP1 (rabbit polyclonal antibody, 1:500) was used as the primary antibody. Staining in the absence of the primary antibody provided the negative control. The staining on each slide was evaluated by one researcher with two independent observations. Samples were blinded to clinicopathologic data and patient outcomes during observation. Immunoreactivity was scored semiquantitatively according to the estimated percentage of positive tumor cells (1, <50% reacting cells; 2, 50–80% reacting cells; 3, >80%) and intensity (1, weaker than the intensity of surface staining in the islet of Langerhans; 2, equal to the intensity of the islet of Langerhans; 3, stronger than the intensity of the islet of Langerhans). The slides, whose islet of Langerhans was not significantly stained, were considered to be in bad condition and were not evaluated. A total immunohistochemical score was calculated by summing the percentage score and the intensity score. The quantity of CDCP1 expression was classified into two groups by the total score (low group, 2–4; high group, 5 and 6).

Statistical analysis

We used the StatView software and SAS version 9.1.3 (SAS Institute, Inc.) for statistical analyses. Cochran-Armitage trend test and χ^2 test were used to assess the association between CDCP1 expression levels and clinicopathologic parameters (Supplementary Table S2). Kaplan-Meier methods were used to calculate overall survival, and differences in survival curves were evaluated with the log-rank test. The hazard ratios (HR) with 95% confidence intervals (CI) of the CDCP1 high-expression effect were estimated using univariate and multivariate Cox's proportional hazards model (Table 1). P values of <0.05 were considered to be statistically significant.

Results

CDCP1 expression is correlated with prognosis of patients with pancreatic cancer

During the screening for the protein expression of CDCP1 in various cancer cell lines, we noticed that CDCP1 is highly expressed and phosphorylated at tyrosines in most pancreatic cell lines (Fig. 1A). CDCP1 is also expressed in other cancer cells such as lung cancers and gastric cancers as we previously reported, whereas it is not expressed in some cancers such as neuroblastomas (data not shown). We further examined CDCP1 expression in human pancreatic cancer tissues by immunohistochemical analysis. Both well-differentiated and poorly differentiated types of pancreatic cancers were significantly stained with the CDCP1 antibody whereas normal pancreatic ducts were not obviously stained (Fig. 1B, a and b). CDCP1 staining was also detected in the perineural invasion site and at sites of lymph node metastasis (Fig. 1B, c–e). Expression levels of CDCP1 in poorly differentiated cancers are generally higher than in well-differentiated types, especially at invasion sites and metastatic loci. CDCP1 protein expression was examined in surgical specimens from 158 patients with pancreatic cancer. Expression levels of CDCP1 were evaluable in 145 cases, and they were classified into the low-expressing (63.4%, $n = 92$) and high-expressing (36.6%, $n = 53$) groups, as described in Materials and Methods. There were no significant associations in the clinicopathologic parameters between CDCP1 expression groups (Supplementary Table S2). The Kaplan-Meier plots also showed that there was a significant difference in overall survival rates ($P = 0.0391$) between groups with high and low CDCP1 expression (Fig. 1C). The effect of CDCP1 expression on overall survival is similar between univariate and multivariate analyses (Table 1).

Tyrosine-phosphorylated CDCP1 regulates cell migration and invasion

As pancreatic cancer cells with high metastatic potential, such as BxPC3 and CFPAC1, seemed to show relatively high phosphorylation levels of CDCP1 at tyrosines (Fig. 1A), we analyzed the role of phosphorylated CDCP1 in the invasion and metastasis of pancreatic cancers. Localization of CDCP1 was mainly detected at cell-cell contact in human tissue samples (Fig. 1B). CDCP1 was also expressed at cell-cell contact

Published OnlineFirst May 25, 2010; DOI:10.1158/0008-5472.CAN-10-0220

Table 1. Univariate and multivariate analyses of prognostic factors for overall survival

	Overall survival			
	Univariate		Multivariate	
	HR (95% CI)	*P*	HR (95% CI)	*P*
Stage*	1.549 (1.275–1.883)	<0.0001	1.458 (1.185–1.795)	0.0004
Primary tumor*	2.833 (1.403–5.718)	0.0037	—	—
Regional lymph nodes*	2.963 (1.592–5.515)	0.0006	—	—
Distant metastasis*	1.994 (1.166–3.408)	0.0117	—	—
Histology†‡	1.340 (0.997–1.801)	0.0525		
Lymphatic invasion (ly0 + ly1 or ly2 + ly3)†	1.954 (1.381–2.765)	0.0002	1.507 (0.977–2.325)	0.0639
Venous invasion (v0 + v1 or v2 + v3)†	1.536 (1.093–2.160)	0.0136	1.308 (0.861–1.987)	0.2084
Intrapancreatic nerve invasion (n0 + n1 or n2 + n3)†	1.340 (0.953–1.884)	0.0923		
Spread within the main pancreatic duct [mpd (–) or mpd (b) + (+)]†	1.065 (0.679–1.668)	0.7848		
CDCP1	1.470 (1.017–2.125)	0.0404	1.482 (1.022–2.150)	0.0381

Abbreviations: mpd, main pancreatic duct; b, borderline.
*Classified according to the classification of International Union Against Cancer.
†Classified according to the classification of pancreatic carcinoma of Japan Pancreas Society.
‡Classified according to the classification of WHO.

in pancreatic cancer cell lines, whereas much lower expression was detected at the free edges of cells (Supplementary Fig. S1).

Suppression of CDCP1 expression by siRNA strongly inhibited cell migration and invasion of pancreatic cancer cells (Fig. 2A; Supplementary Fig. S2). Similar to the previous report in lung cancer cells (5), downregulation of CDCP1 in pancreatic cancer cells had no significant effect on the phosphorylation of AKT and extracellular signal-regulated kinase 1/2, which are essential components of the growth factor signaling pathway mediating cell survival, proliferation, and motility (data not shown). For rescue experiments, vectors expressing wild-type CDCP1 and Y734F mutant CDCP1, which lacks the SFKs-binding site, were designed to contain silent mutations to be resistant to siRNA for CDCP1 as shown in Fig. 2B (CDCP1 res-F and Y734F res-F, respectively). Tyrosine phosphorylation of CDCP1 is shown to be attenuated in Y734F mutant through dissociation from SFKs (Supplementary Fig. S3). After suppression by CDCP1 siRNA, CDCP1 expression was restored by transfection of either CDCP1 res-F or Y734F res-F constructs in BxPC3 as expected (Fig. 2C). Both migration and invasion were recovered by the CDCP1 res-F construct to the level of original BxPC3 cells, but not by the Y734F res-F mutant (Fig. 2D), suggesting that CDCP1 regulates migration and invasion in a tyrosine phosphorylation–dependent manner.

Tyrosine-phosphorylated CDCP1 promotes ECM degradation

Because the biological role of CDCP1 in invasion is totally unknown, we first examined whether CDCP1 influences ECM degradation of cancer cells. Loss of CDCP1 decreased the ability to degrade fluorescence-conjugated collagen on cover glasses (Fig. 3A), whereas it caused no significant effect on the degree of cell-ECM attachment (data not shown). To quantify the ability of ECM degradation, cells that are >50% covered by dark area with degraded collagen were counted, and the ratio to the total number of cells was calculated. This ratio of degradation showed 40% to 90% decrease in BxPC3 and Capan1 by suppression of CDCP1 (Fig. 3B). Protease secretion was then analyzed by zymography to identify factor (s) that regulates ECM degradation. Suppression of CDCP1 attenuated gelatin degradation bands at ~90 kDa detected in culture medium of BxPC3 and CFPAC1 (Fig. 3C, top; Supplementary Fig. S4). The bands at ~90 kDa in the zymogram correspond to the molecular size of MMP-9, a major MMP expressed in invasive cancer, and were actually detected by Western blotting using the anti–MMP-9 antibody (Fig. 3C, bottom left). Treatment of MMP inhibitor II, which inhibits a series of MMPs including MMP-9, suppressed the bands at ~90 kDa in both BxPC3 and HT1080, which is already known to secrete MMP-9 (Fig. 3C, bottom right), whereas the bands at ~60 kDa, presumably MMP-2, were not inhibited in HT1080 cells. The quantity of MMP-9 mRNA was not affected by CDCP1 siRNA (data not shown). These results indicate that CDCP1 controls ECM degradation through secretion of proteases, including MMP-9, in pancreatic cancer cells.

CDCP1 induces activation of PKCδ through tyrosine phosphorylation of PKCδ

It was shown in pancreatic cancer cell lines that tyrosine phosphorylation of CDCP1 at Tyr^{734} triggers its association with a downstream target PKCδ, recruitment of PKCδ to the CDCP1-SFKs complex, and tyrosine phosphorylation of PKCδ (Fig. 2C; Supplementary Fig. S3), which is required for anoikis resistance of cancer cells (5). Suppression of PKCδ inhibited cell migration and invasion (Supplementary Fig. S5)

Published OnlineFirst May 25, 2010; DOI:10.1158/0008-5472.CAN-10-0220

and also blocked ECM degradation and protease secretion in BxPC3 and CFPAC1 (Fig. 4A; data not shown). The overexpression of the HA-tagged C2 domain of PKCδ, which was designed to block the CDCP1-PKCδ interaction (4, 5), resulted in decrease of migration and invasion of Capan1 cells (Fig. 4B), suggesting the CDCP1-PKCδ association is essential for these characteristics. Moreover, the overexpression of Y734F-F mutant in BxPC3 decreased ECM degradation and the secretion of proteases, including MMP-9 (Fig. 4C). This Y734F-F mutant suppressed tyrosine phosphorylation of PKCδ without significantly affecting the phosphorylation states of wild-type CDCP1 (Fig. 4C), possibly by interfering the extracellular signal, which might also modulate CDCP1-PKCδ signal in a dominant-negative manner. Phosphorylation of PKCδ at Thr^{505}, which was reported to indicate kinase activity of PKCδ (16), was examined by using a phosphospecific antibody. Phosphorylation of PKCδ at Thr^{505} was actually induced by treatment of phorbol 12-myristate 13-acetate (PMA), an activator of PKCs, whereas it was reduced by suppression of CDCP1 expression (Fig. 4D). It was indicated that tyrosine phosphorylation of PKCδ by CDCP1 affects the kinase activity of PKCδ.

Cortactin is a candidate protein downstream of the CDCP1-PKCδ pathway in cell migration and invasion

Treatment of CDCP1 siRNA did not cause significant effects on the phosphorylation status of several signaling proteins such as paxillin, focal adhesion kinase, and adducin, which were reported as downstream molecules of PKCδ (data not shown). On the other hand, we discovered that cortactin, which has been detected as one of the major substrates for SFKs and has been reported to play an essential

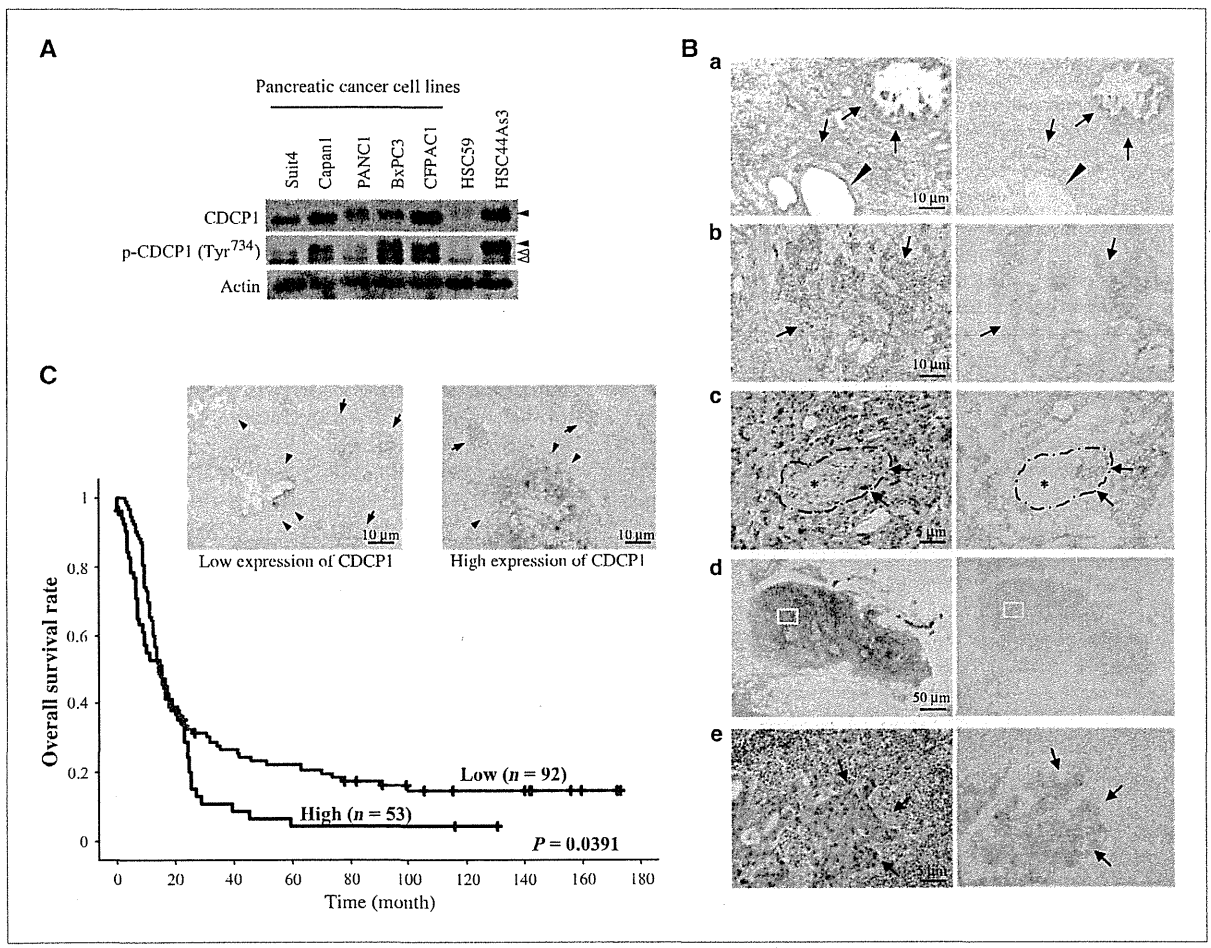

Figure 1. CDCP1 expression is correlated with prognosis of patients with pancreatic cancer. A, expression and tyrosine phosphorylation of CDCP1 in pancreatic cancer and noninvasive (HSC59) or invasive (HSC44As3) gastric cancer cell lines. Black arrowheads, CDCP1; white arrowheads, cross-reactive bands. B, CDCP1 expression in human pancreatic cancer tissues. Left, H&E staining; right, immunohistochemistry with anti-CDCP1 antibody. a, black arrowhead, normal pancreatic cells; black arrow, well-differentiated types of pancreatic cancers. b, poorly differentiated types of pancreatic cancers; c, perineural invasion (dotted line, epineurium; *, nerve); d and e, lymph node metastasis. e, enlargements of yellow squares in d. Magnifications, ×20 (d), ×100 (a and b), and ×200 (c and e). C, black arrowheads, pancreatic cancer; black arrows, islet of Langerhans for control staining. Kaplan-Meier plots of overall survival of patients with pancreatic cancer. High, CDCP1 high-expression group; Low, CDCP1 low-expression group.

Published OnlineFirst May 25, 2010; DOI:10.1158/0008-5472.CAN-10-0220

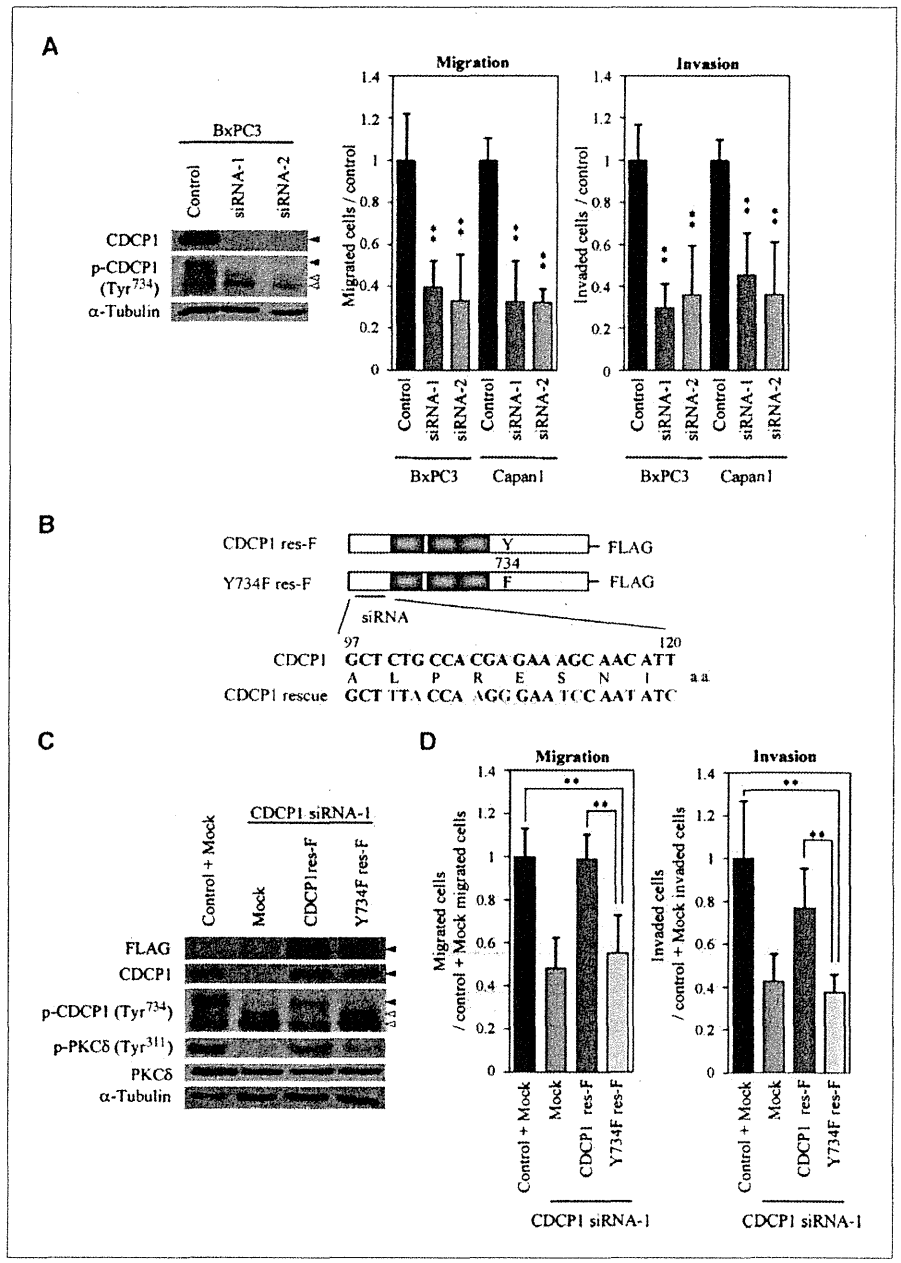

Figure 2. CDCP1 regulates migration and invasion in a tyrosine phosphorylation–dependent manner. A, left, BxPC3 cells treated with CDCP1 siRNAs were used for immunoblotting with the indicated antibodies; right, migration and invasion assay of BxPC3 and Capan1 (4.0×10^4 cells) treated with CDCP1 siRNAs. Black arrowheads, CDCP1; white arrowheads, cross-reactive bands. B, schematic structure of CDCP1 and CDCP1 rescue mutant tagged with FLAG (CDCP1 res-F and Y734F res-F). The DNA base sequence that is not suppressed by CDCP1 siRNA is described. C, BxPC3 cells were treated with each siRNA and, 48 h later, transfected with the indicated plasmid. Cancer cells were used for immunoblotting with the indicated antibodies. Black arrowheads, CDCP1; white arrowheads, cross-reactive bands. D, migration and invasion assay using CDCP1 rescue mutant. BxPC3 cells treated with either control siRNA + pcDNA3.1 + pEGFP (bars, control + mock) or CDCP1 siRNA + each plasmid DNA + pEGFP (bars, mock, CDCP1 res-F, Y734F res-F) were used for each assay. Only migrated and invaded cells expressing green fluorescent protein (GFP) were counted using a fluorescence microscope. Columns, mean; bars, SD. The asterisks indicate statistically significant differences from the cells compared with control siRNA or control siRNA + Mock. *, $P < 0.05$; **, $P < 0.005$.

role in cell migration and invasion (17–19), was localized with CDCP1 and PKCδ at cell-cell contact in BxPC3 (Fig. 5A), and showed physical association with PKCδ through immunoprecipitation (Fig. 5B). Interestingly, suppression of CDCP1 disrupted the physical association between PKCδ and cortactin. On the other hand, tyrosine phosphorylation of cortactin was not affected by suppression of CDCP1 (Supplementary Fig. S6). Suppression of cortactin decreased migration and invasion in BxPC3 (Fig. 5C), as also reported in other cell types (20, 21), whereas it did not suppress ECM degradation (Fig. 5D) and gelatin degradation by proteases in the zymogram (data not shown) in BxPC3 and CFPAC1 cells. These results suggest that cortactin might be one of the mediators of the CDCP1-PKCδ signaling complex in cancer cell migration but not in the ECM degradation.

Discussion

CDCP1 was originally identified as a membrane protein selectively expressed in the surface of metastatic cancers such as colon and lung cancers. It was later shown that CDCP1 is a potent substrate of SFKs *in vitro*, and our previous analysis

Published OnlineFirst May 25, 2010; DOI:10.1158/0008-5472.CAN-10-0220

revealed that phosphorylation of CDCP1 by SFKs is essential for the anoikis resistance, which supports distant metastasis of solid cancers. In this study, we showed that CDCP1 is a significant prognostic factor that predicts the overall survival of patients with pancreatic cancer. We further showed for the first time that CDCP1-PKCδ signaling plays a crucial role in cell migration and ECM degradation in pancreatic cancer cells.

CDCP1 mRNA and protein expressions were found in various human solid cancers, including colon, lung, and breast cancers (1, 7, 22). CDCP1 was recently shown to be a prognostic factor of lung adenocarcinoma and renal cell carcinoma by using a large-scale analysis of CDCP1 expression in tumor samples (7, 8). By histologic analysis using human pancreatic cancer tissues, CDCP1 expression was detected not only in the original lesion but also in lymph node metastasis and perineural invasion (Fig. 1B). Pancreatic cancer is one of the most frequent causes of cancer-related deaths worldwide. The poor prognosis is attributed to the high incidence of distant metastasis at the point of diagnosis and the highly invasive nature of this cancer. In that sense, it is important that the patients with high CDCP1 expression showed significantly worse overall survival on both univariate and multivariate analyses, suggesting that it might be a novel and independent prognostic factor of pancreatic cancer (Table 1). The individual clinicopathologic factors were not statistically significantly correlated with CDCP1 expression, which may be due to remarkably short overall survival in patients with pancreatic cancers compared with those with renal cell carcinomas or lung cancers. Although general prognostic markers such as p16, MMP-7, and vascular endothelial growth factor are also applicable to patients with pancreatic cancer (23), CDCP1 is an essential marker of poor

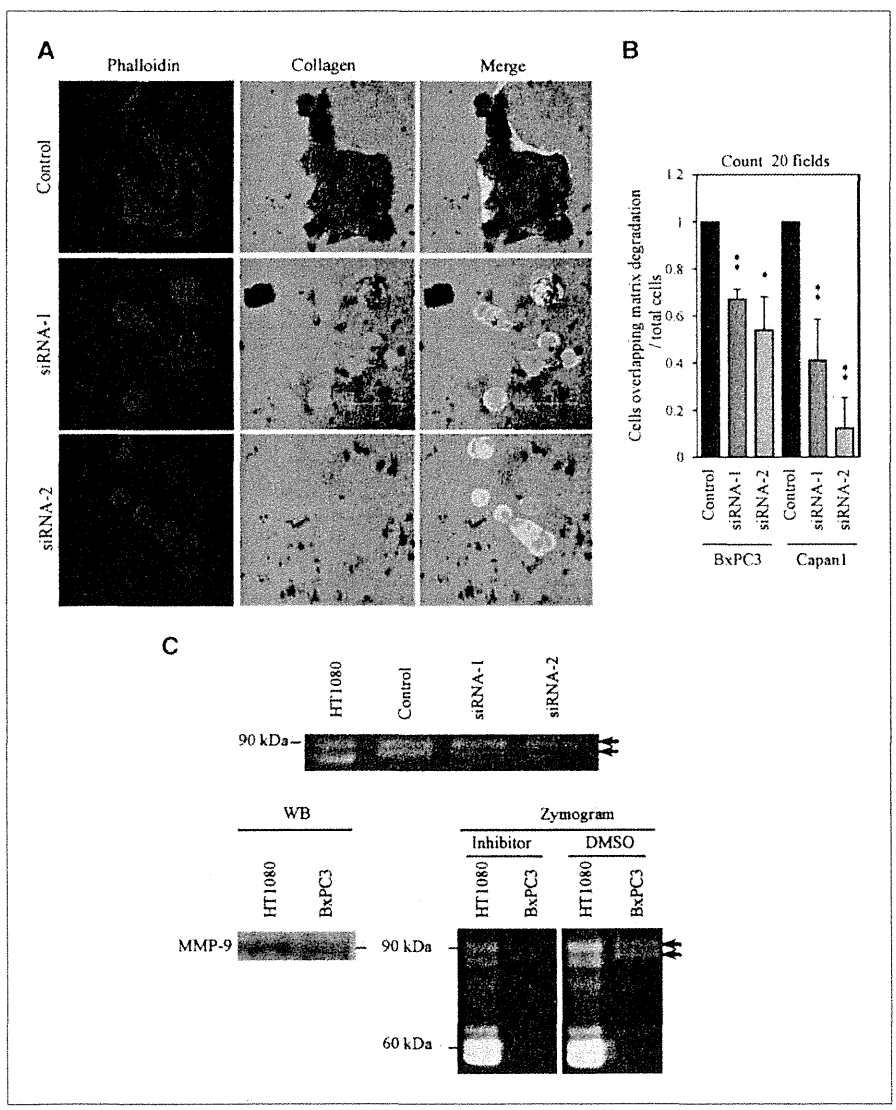

Figure 3. Tyrosine-phosphorylated CDCP1 promotes ECM degradation. A, BxPC3 cells transfected with CDCP1 siRNAs were incubated on covered glasses with fluorescein-conjugated collagen and stained with phalloidin to identify actin filaments. ECM degradation is identified as the dark area. B, quantification of ECM degradation. Cells overlapping the dark area, occupying more than half of the cell area, were counted. Columns, mean; bars, SD. The asterisks indicate statistically significant differences from the cells compared with control siRNA. *, $P < 0.05$; **, $P < 0.005$. C, top, gelatin zymography in BxPC3 transfected with CDCP1 siRNAs. Left, culture medium using BxPC3 and HT1080 cultures was concentrated and analyzed by Western blotting (WB) with the anti–MMP-9 antibody; right, zymogram of samples treated with MMP inhibitor II and DMSO. Black arrows, gelatin degradation.

Published OnlineFirst May 25, 2010; DOI:10.1158/0008-5472.CAN-10-0220

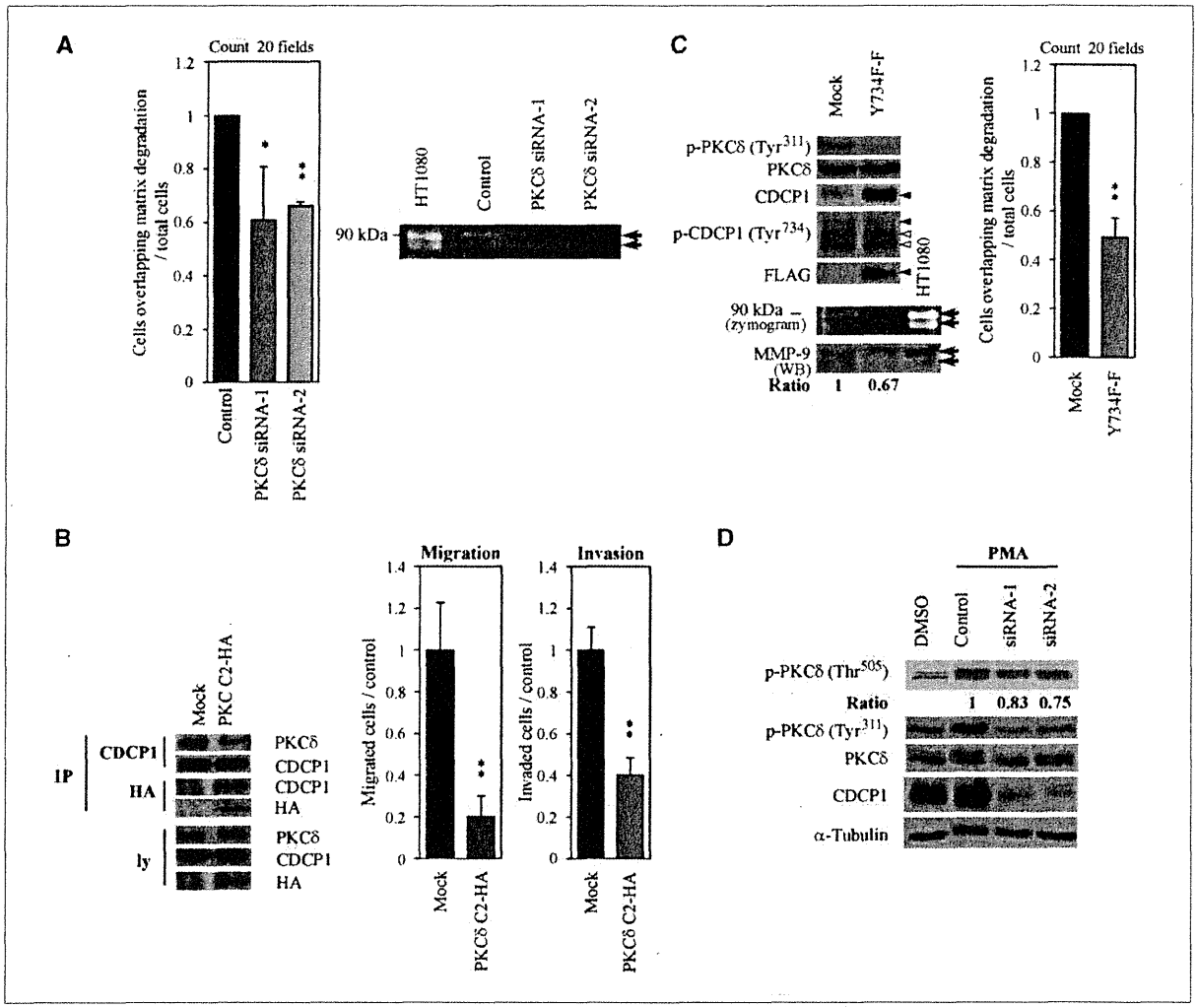

Figure 4. CDCP1 regulates migration and invasion via the PKCδ kinase activity. A, quantification of ECM degradation assay and zymogram of BxPC3 cells transfected with PKCδ siRNAs. Black arrows, MMP-9. B, left, Capan1 cells transfected with the C2 domain of PKCδ tagged with HA (PKCδ C2-HA) or pcDNA3.1 (Mock) were selected by G418. The lysate immunoprecipitated (IP) with anti-CDCP1 or anti-HA antibodies was used for immunoblotting with the indicated antibodies. Right, migration and invasion assay using Capan1 (4.0×10^4 cells) transfected with the indicated plasmids. C, left, top, BxPC3 cells transfected with the CDCP1 mutant (Y734F res-F) or pcDNA3.1 (Mock) were selected by G418 and used for immunoblotting with the indicated antibodies; bottom, culture medium of the BxPC3 was analyzed by gelatin zymography and Western blotting with anti–MMP-9 antibody. Ratio, total MMP-9 of mock or Y734F/total MMP-9 of mock in Western blotting. Right, quantification of ECM degradation of BxPC3. Columns, mean; bars, SD. The asterisks indicate statistically significant differences from the cells transfected with control siRNA or mock. Black arrowheads, CDCP1; white arrowheads, cross-reactive bands; black arrows, MMP-9. *, $P < 0.05$; **, $P < 0.005$. D, BxPC3 cells transfected with CDCP1 siRNAs are cultured in 0.5% FBS for 24 h and treated with 100 nmol/L PMA or DMEM for 20 min at 37°C. The cells were used for immunoblotting with the indicated antibodies. Ratio, [phospho-PKCδ Thr^{505}/PKCδ (each siRNA)]/[phspho-PKCδ Thr^{505}/PKCδ (control siRNA)].

prognosis that is functionally related to particular malignant characteristics such as migration, ECM degradation, and anoikis resistance of cancer cells. This study also indicates that CDCP1 induces ECM degradation through secretion of proteases including MMP-9 (Figs. 3C and 4C). MMP-9 secretion has also been reported in human pancreatic tissue (24, 25) and was also considered to be a potential prognostic factor in pancreatic cancer (26).

A recent observation indicates that CDCP1 protein is expressed in some normal human tissues, such as the colon, breast, and lung, but not in the pancreatic duct (Fig. 1B), whereas the levels of CDCP1 phosphorylation in these normal tissues were much lower than those in cancer cells (27). We previously reported that phosphorylation of CDCP1 at Tyr^{734} is increased during peritoneal dissemination of gastric cancer *in vivo* and that it could promote migration of gastric cancer cells *in vitro* (6). In this study, we showed that phosphorylation of CDCP1 at Tyr^{734} plays a significant role in promotion of cell migration and ECM degradation, in addition to anoikis resistance of cancer cells. Therefore, it is

Published OnlineFirst May 25, 2010; DOI:10.1158/0008-5472.CAN-10-0220

reasonable that not only the expression but also the tyrosine phosphorylation of CDCP1 is required for these characteristics of cancer cells associated with invasion and metastasis.

The complex formation between tyrosine-phosphorylated CDCP1 and PKCδ is required for the promotion of migration and ECM degradation. Our results also suggest that tyrosine phosphorylation of PKCδ, which was triggered by the association with phosphorylated CDCP1 coupled with SFKs, is essential for CDCP1-induced cell migration and ECM degradation. Judging from the levels of phosphorylation at Thr^{505} of PKCδ (Fig. 4D), a putative autophosphorylation site in an activation loop (16), tyrosine phosphorylation of PKCδ by the SFKs-CDCP1 pathway might activate PKCδ. Previous studies on PKCδ have shown that phosphorylation of PKCδ at Tyr^{311} results in enhanced phosphorylation at Thr^{505} (28) and that activation of PKCδ enhances the MMP-9 activity (29). These findings suggest that the formation of the SFKs-CDCP1-PKCδ complex triggered by tyrosine phosphorylation of CDCP1 causes tyrosine phosphorylation of PKCδ and activation of kinase activity of PKCδ, which promotes cell migration and ECM degradation.

We identified cortactin as a binding partner of PKCδ. Cortactin is one of the key molecules that control cell migration and invasion. Some studies have reported that serine phosphorylation, but not tyrosine phosphorylation, of cortactin increases N-WASP binding and facilitates N-WASP–dependent actin polymerization (30, 31). Because the kinase activity of PKCδ (Fig. 4D) and the association of PKCδ and cortactin (Fig. 5B) can be affected by CDCP1, CDCP1 possibly regulates cell migration by altering serine/threonine phosphorylation of cortactin through PKCδ. Unfortunately, this could not be confirmed due to the lack of a good specific

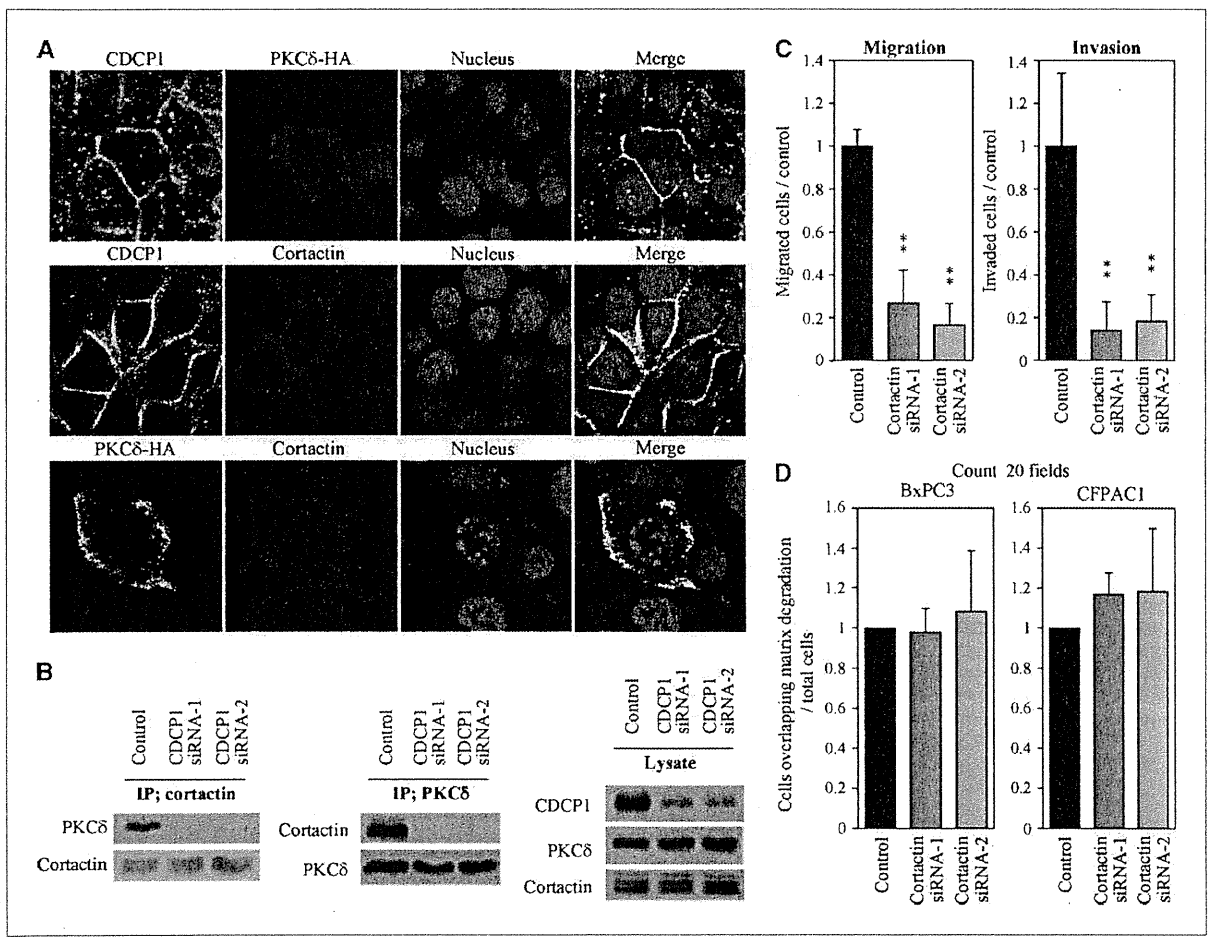

Figure 5. Cortactin, a PKCδ-associated protein, regulates cell migration and invasion. A, top, BxPC3 stained with anti-HA antibody (PKCδ-HA; red) and anti-CDCP1 antibody (green). The nucleus was stained with TOTO3. Middle, BxPC3 stained with anti-CDCP1 antibody (green) and anti-cortactin antibody (red). Bottom, BxPC3 stained with anti-HA antibody (PKCδ-HA; green) and anti-cortactin antibody (red). B, immunoprecipitation with anti-cortactin or anti-PKCδ antibodies in BxPC3 transfected with each siRNA. Samples were immunoblotted with the indicated antibodies. C, migration and invasion assay of BxPC3 (1.0×10^4 cells) transfected with cortactin siRNAs. Columns, mean; bars, SD. The asterisks indicate differences from cells treated with control siRNA. *, $P < 0.05$; **, $P < 0.005$. D, quantification of ECM degradation of protease in BxPC3.

Published OnlineFirst May 25, 2010; DOI:10.1158/0008-5472.CAN-10-0220

antibody against serine/threonine-phosphorylated cortactin. Cortactin has also been reported to play a role in the function of invadopodia in several cancers (32, 33), although a structure similar to invadopodia was not found in the pancreatic cancer cells used in this study. Loss of cortactin did not suppress ECM degradation and protease secretion in pancreatic cancer cells, suggesting that some molecules other than cortactin might be regulating ECM degradation under the control of CDCP1, whereas cortactin is involved in CDCP1-induced migration of cells possibly through regulation of actin dynamics.

As CDCP1 binds the regulatory domain of SFKs (5), there is a possibility that CDCP1 controls the activity of SFKs by unfolding these proteins. Positive correlation between CDCP1 expression and Tyr^{418} phosphorylation, which indicates autophosphorylation activity of SFKs, was obtained in BxPC3 cells (data not shown), whereas no clear correlation was obtained in other pancreatic cell lines. Further study will be required to understand the functional association between SFKs and CDCP1, including identification of other modulators of association.

Collectively, CDCP1 is a novel prognostic factor of pancreatic cancer, and inhibition of a specific cellular signal originating from the expression of phosphorylated CDCP1 has been shown to regulate cell migration, invasion, and ECM degradation in pancreatic cancer cells. Because early clinical diagnosis of pancreatic cancer is difficult, invasion or metastasis to other organs frequently precedes diagnosis. In addition to its diagnostic usefulness as a membrane protein, CDCP1 might be an optimal therapeutic target of invasive and metastatic pancreatic cancers alone or combined with general chemotherapy drugs.

Disclosure of Potential Conflicts of Interest

No potential conflicts of interest were disclosed.

Acknowledgments

We thank Aya Kuchiba and Seiichiro Yamamoto for advice and discussion about the statistics.

Grant Support

Grant-in-Aid for Cancer Research and Grant-in-Aid for Scientific Research from the Ministry of Education, Culture, Science and Technology of Japan for the third-term Comprehensive Ten-Year Strategy for Cancer Control.

The costs of publication of this article were defrayed in part by the payment of page charges. This article must therefore be hereby marked *advertisement* in accordance with 18 U.S.C. Section 1734 solely to indicate this fact.

Received 01/20/2010; revised 04/13/2010; accepted 04/14/2010; published OnlineFirst 05/25/2010.

References

1. Scherl-Mostageer M, Sommergruber W, Abseher R, Hauptmann R, Ambros P, Schweifer N. Identification of a novel gene, CDCP1, overexpressed in human colorectal cancer. Oncogene 2001;20:4402–8.
2. Hooper JD, Zijlstra A, Aimes RT, et al. Subtractive immunization using highly metastatic human tumor cells identifies SIMA135/CDCP1, a 135 kDa cell surface phosphorylated glycoprotein antigen. Oncogene 2003;22:1783–94.
3. Brown TA, Yang TM, Zaitsevskaia T, et al. Adhesion or plasmin regulates tyrosine phosphorylation of a novel membrane glycoprotein p80/gp140/CUB domain-containing protein 1 in epithelia. J Biol Chem 2004;279:14772–83.
4. Benes CH, Wu N, Elia AE, Dharia T, Cantley LC, Soltoff SP. The C2 domain of PKCδ is a phosphotyrosine binding domain. Cell 2005; 121:271–80.
5. Uekita T, Jia L, Narisawa-Saito M, Yokota J, Kiyono T, Sakai R. CUB domain-containing protein 1 is a novel regulator of anoikis resistance in lung adenocarcinoma. Mol Cell Biol 2007;27:7649–60.
6. Uekita T, Tanaka M, Takigahira M, et al. CUB-domain-containing protein 1 regulates peritoneal dissemination of gastric scirrhous carcinoma. Am J Pathol 2008;172:1729–39.
7. Ikeda J, Oda T, Inoue M, et al. Expression of CUB domain containing protein (CDCP1) is correlated with prognosis and survival of patients with adenocarcinoma of lung. Cancer Sci 2009;100:429–33.
8. Awakura Y, Nakamura E, Takahashi T, et al. Microarray-based identification of CUB-domain containing protein 1 as a potential prognostic marker in conventional renal cell carcinoma. J Cancer Res Clin Oncol 2008;134:1363–9.
9. Uekita T, Gotoh I, Kinoshita T, et al. Membrane-type 1 matrix metalloproteinase cytoplasmic tail-binding protein-1 is a new member of the Cupin superfamily. A possible multifunctional protein acting as an invasion suppressor down-regulated in tumors. J Biol Chem 2004; 279:12734–43.
10. Uekita T, Itoh Y, Yana I, Ohno H, Seiki M. Cytoplasmic tail-dependent internalization of membrane-type 1 matrix metalloproteinase is important for its invasion-promoting activity. J Cell Biol 2001; 155:1345–56.
11. Jia L, Uekita T, Sakai R. Hyperphosphorylated cortactin in cancer cells plays an inhibitory role in cell motility. Mol Cancer Res 2008; 6:654–62.
12. Sobin L, Witteknd C. TNM classification of malignant tumors. 6th ed. New York: Wiley-Liss; 2002, p. 93–6.
13. Japan Pancreatic Society. Classification of pancreatic carcinoma. 2nd English ed. Tokyo: Kanehara & Co.; 2003.
14. Klöppel G, Hruban RH, Longnecker DS, et al. Ductal adenocarcinoma of the pancreas. In: Hamilton SR, Aaltonen LA, editors. Pathology and genetics. Tumours of the digestive system. World Health Organization classification of tumours. Lyon (France): IARC Press; 2000, p. 221–30.
15. Takahashi Y, Hiraoka N, Onozato K, et al. Solid-pseudopapillary neoplasms of the pancreas in men and women: do they differ? Virchows Arch 2006;448:561–9.
16. Rybin VO, Sabri A, Short J, Braz JC, Molkentin JD, Steinberg SF. Cross-regulation of novel protein kinase C (PKC) isoform function in cardiomyocytes. Role of PKCε in activation loop phosphorylations and PKCδ in hydrophobic motif phosphorylations. J Biol Chem 2003; 278:14555–64.
17. Huang C, Liu J, Haudenschild CC, Zhan X. The role of tyrosine phosphorylation of cortactin in the locomotion of endothelial cells. J Biol Chem 1998;273:25770–6.
18. Huang J, Asawa T, Takato T, Sakai R. Cooperative roles of Fyn and cortactin in cell migration of metastatic murine melanoma. J Biol Chem 2003;278:48367–76.
19. Bryce NS, Clark ES, Leysath JL, Currie JD, Webb DJ, Weaver AM. Cortactin promotes cell motility by enhancing lamellipodial persistence. Curr Biol 2005;15:1276–85.
20. van Rossum AG, Moolenaar WH, Schuuring E. Cortactin affects cell migration by regulating intercellular adhesion and cell spreading. Exp Cell Res 2006;312:1658–70.
21. Yamaguchi H, Condeelis J. Regulation of the actin cytoskeleton in cancer cell migration and invasion. Biochim Biophys Acta 2007; 1773:642–52.
22. Bühring HJ, Kuçi S, Conze T, et al. CDCP1 identifies a broad

Published OnlineFirst May 25, 2010; DOI:10.1158/0008-5472.CAN-10-0220

spectrum of normal and malignant stem/progenitor cell subsets of hematopoietic and nonhematopoietic origin. Stem Cells 2004;22: 334–43.
23. Tonini G, Pantano F, Vincenzi B, Gabbrielli A, Coppola R, Santini D. Molecular prognostic factors in patients with pancreatic cancer. Expert Opin Ther Targets 2007;11:1553–69.
24. Gress TM, Müller-Pillasch F, Lerch MM, Friess H, Büchler M, Adler G. Expression and *in-situ* localization of genes coding for extracellular matrix proteins and extracellular matrix degrading proteases in pancreatic cancer. Int J Cancer 1995;62:407–13.
25. Hirata M, Itoh M, Tsuchida A, Ooishi H, Hanada K, Kajiyama G. Cholecystokinin receptor antagonist, loxiglumide, inhibits invasiveness of human pancreatic cancer cell lines. FEBS Lett 1996;383:241–4.
26. Mroczko B, Lukaszewicz-Zajac M, Wereszczynska-Siemiatkowska U, et al. Clinical significance of the measurements of serum matrix metalloproteinase-9 and its inhibitor (tissue inhibitor of metalloproteinase-1) in patients with pancreatic cancer: metalloproteinase-9 as an independent prognostic factor. Pancreas 2009;38:613–8.
27. Wong CH, Baehner FL, Spassov DS, et al. Phosphorylation of the SRC epithelial substrate Trask is tightly regulated in normal epithelia but widespread in many human epithelial cancers. Clin Cancer Res 2009;15:2311–22.
28. Rybin VO, Guo J, Gertsberg Z, Elouardighi H, Steinberg SF. Protein kinase Cε (PKCε) and Src control PKCδ activation loop phosphorylation in cardiomyocytes. J Biol Chem 2007;282:23631–8.
29. Park SK, Hwang YS, Park KK, Park HJ, Seo JY, Chung WY. Kalopanax saponin A inhibits PMA-induced invasion by reducing matrix metalloproteinase-9 via PI3K/Akt- and PKCδ-mediated signaling in MCF-7 human breast cancer cells. Carcinogenesis 2009; 30:1225–33.
30. Campbell DH, Sutherland RL, Daly RJ. Signaling pathways and structural domains required for phosphorylation of EMS1/cortactin. Cancer Res 1999;59:5376–85.
31. Martinez-Quiles N, Ho HY, Kirschner MW, Ramesh N, Geha RS. Erk/Src phosphorylation of cortactin acts as a switch on-switch off mechanism that controls its ability to activate N-WASP. Mol Cell Biol 2004;24:5269–80.
32. Bowden ET, Barth M, Thomas D, Glazer RI, Mueller SC. An invasion-related complex of cortactin, paxillin and PKCμ associates with invadopodia at sites of extracellular matrix degradation. Oncogene 1999; 18:4440–9.
33. Onodera Y, Hashimoto S, Hashimoto A, et al. Expression of AMAP1, an ArfGAP, provides novel targets to inhibit breast cancer invasive activities. EMBO J 2005;24:963–73.

British Journal of Cancer (2010) 103, 1057–1065

www.bjcancer.com

Tumour necrosis is a postoperative prognostic marker for pancreatic cancer patients with a high interobserver reproducibility in histological evaluation

N Hiraoka*[,1], Y Ino[1], S Sekine[1], H Tsuda[2], K Shimada[3], T Kosuge[3], J Zavada[4], M Yoshida[2], K Yamada[2], T Koyama[2] and Y Kanai[1]

[1]Pathology Division, National Cancer Center Research Institute, 5-1-1 Tsukiji, Chuo-ku, Tokyo 104-0045, Japan; [2]Clinical Laboratory Division, National Cancer Center Hospital, 5-1-1 Tsukiji, Chuo-ku, Tokyo 104-0045, Japan; [3]Hepato-Biliary and Pancreatic Surgery Division, National Cancer Center Hospital, 5-1-1 Tsukiji, Chuo-ku, Tokyo 104-0045, Japan; [4]Institute of Organic Chemistry and Biochemistry, Flemingovo nam.2, 166 10 Prague 6, Czech Republic

BACKGROUND: Tumour necrosis reflects the presence of hypoxia, which can be indicative of an aggressive tumour phenotype. The aim of this study was to investigate whether histological necrosis is a useful predictor of outcome in patients with pancreatic ductal carcinoma (PDC).

METHODS: We reviewed histopathological findings in 348 cases of PDC in comparison with clinicopathological information. We counted small necrotic foci (micronecrosis) as necrosis, in addition to massive necrosis that had been only defined as necrosis in previous studies. The reproducibility of identifying histological parameters was tested by asking five independent observers to blindly review 51 examples of PDC.

RESULTS: Both micronecrosis and massive necrosis corresponded to hypoxic foci expressing carbonic anhydrase IX detected by immunohistochemistry. Multivariate survival analysis showed that histological necrosis was an independent predictor of poor outcome in terms of both disease-free survival (DFS) and disease-specific survival (DSS) of PDC patients. In addition, metastatic status, and lymphatic, venous, and intrapancreatic neural invasion were independent prognostic factors for shorter DFS and metastatic status, margin status, lymphatic invasion, and intrapancreatic neural invasion were independent prognostic factors for DSS. The interobserver reproducibility of necrosis identification among the five independent observers was 'almost perfect' (κ-value of 0.87).

CONCLUSION: Histological necrosis is a simple, accurate, and reproducible predictor of postoperative outcome in PDC patients.

British Journal of Cancer (2010) **103,** 1057–1065. doi:10.1038/sj.bjc.6605854 www.bjcancer.com
Published online 24 August 2010

Keywords: necrosis; pancreatic cancer; prognostic factor; interobserver reproducibility; hypoxia

Pancreatic cancer (pancreatic ductal carcinoma (PDC)) is the fourth and fifth leading cause of cancer-related death in the United States and Japan, respectively (Center for Cancer Control and Information Services and National Cancer Center, 2009; Jemal *et al*, 2009). Because of its aggressive growth and early metastatic dissemination, the overall 5-year survival rate for patients with pancreatic cancer is 3–5%, and that of patients treated by curative resection is 15–25% (Klöppel *et al*, 2000; Lim *et al*, 2003; Hruban *et al*, 2007; Jemal *et al*, 2009). The mortality rate has not shown any obvious improvement for decades. The development of predictive biomarkers to assist the selection of patient subsets is useful for studies aimed at reducing the mortality of PDC patients, especially in phase clinical studies evaluating various therapeutic approaches (Philip *et al*, 2009).

Several histopathological parameters such as tumour size (Yeo *et al*, 1995; Sohn *et al*, 2000; Lim *et al*, 2003; Shimada *et al*, 2006), tumour histological grade (Luttges *et al*, 2000; Adsay *et al*, 2005), lymph nodal metastasis (Trede *et al*, 1990; Lim *et al*, 2003; Schnelldorfer *et al*, 2008), and lymphatic, venous (Luttges *et al*, 2000; Takai *et al*, 2003), and neural invasion (Mitsunaga *et al*, 2005, 2007) have been proposed as hallmarks predictive of postoperative outcome in patients with PDC. Stage is the most important prognosticator (Klöppel *et al*, 2000; Hruban *et al*, 2007), although majority of resectable cases were classified into advanced stage, stage IIB of the International Union Against Cancer (UICC) tumour–node–metastasis (TNM) classification and were not able to be stratified more precisely. Histopathological evaluation of PDC can be performed using routine diagnostic techniques in pathology departments without any additional equipment or special expertise. The predictive values of the above mentioned parameters are sometimes controversial and complex, and some have problems related to interobserver reproducibility. To avoid these pitfalls and to stratify PDCs in a distinct and objective manner, molecular or genetic markers have been developed, although these often require special equipment or expertise and cannot usually be performed on a routine basis. Therefore, simpler, more reproducible, and easily assessable histopathological predictors are needed.

*Correspondence: Dr N Hiraoka; E-mail: nhiraoka@ncc.go.jp
Received 24 May 2010; revised 14 July 2010; accepted 20 July 2010; published online 24 August 2010

Hypoxia is a common feature of human cancers, which induces a transcription programme mediated mainly by hypoxia-inducible factor-1α (HIF-1α) that promotes aggressive tumour phenotype (Harris, 2002; Vaupel and Mayer, 2007; Bristow and Hill, 2008). It is a prognostic indicator in many solid tumours (Vaupel and Mayer, 2007), and is often detected by examining the expression of carbonic anhydrase IX (CAIX) (Chia *et al*, 2001), which is a regulator of cellular pH and its expression is induced by HIF-1α (Harris, 2002; Bristow and Hill, 2008). Intratumoural hypoxia is reflected histologically by the presence of necrosis, which has also been reported to be a prognostic factor in patients with breast (Gilchrist *et al*, 1993) and bladder (Ord *et al*, 2007) cancers. Hypoxia is evident in PDCs, in which expression of HIF-1α and CAIX has been detected in 60–70% and 78% of cases, respectively (Kitada *et al*, 2003; Couvelard *et al*, 2005; Sun *et al*, 2007), whereas histological necrosis has been found in only 30–40% of PDCs in previous studies (Couvelard *et al*, 2005; Mitsunaga *et al*, 2005). Neither large-scale study nor multivariate survival study has been performed to evaluate prognostic value of hypoxia in PDC patients.

In this study, we found that necrotic areas were present in more than 60% of PDCs when small necrotic foci were taken into account. We also found that CAIX were expressed in and around these necrotic lesions, indicating that these areas were in a condition of hypoxia. Therefore, detection of necrosis using our definition may offer a chance of stratifying PDC patients for tissue hypoxia more accurately. In this study, with the aim of investigating whether histologically evident necrosis is useful for prediction of patient outcome among various histopathological parameters, and we reviewed histopathological findings in 348 cases of PDC in comparison with clinicopathological information.

MATERIALS AND METHODS

Study population

This study was approved by the Ethics Committee of the National Cancer Center, Japan. Clinical and pathological data were obtained through a detailed retrospective review of the medical records of all 348 patients with ductal carcinoma of the pancreas that had undergone initial surgical resection between 1990 and 2005 at the National Cancer Center Hospital. None of the patients had received any previous therapy. All patients received standard therapy appropriate for their clinical stages. The operative procedures included 228 pancreatoduodenectomies or pylorus-preserving pancreatoduodenectomies, 104 distal pancreatectomies, and 16 total pancreatectomies. Along with tumour extension, lymphadenectomy was performed at the hepatoduodenal ligament and around the abdominal aorta. All the patients included in this study underwent macroscopic curative resection, which was defined as the macroscopic removal of all gross tumours without liver metastases, macroscopic peritoneal dissemination, bulky lymph node involvement, or apparent tumour invasion around the common hepatic or superior mesenteric arteries after routine examination using intraoperative ultrasonography. All of the cases were conventional ductal carcinomas and adenocarcinomas originating in intraductal papillary mucinous neoplasms or mucinous cystic neoplasms were excluded. Secondary tumours and postneoadjuvant cases were also excluded. The clinicopathological characters of the patients were summarized in Table 1. All M1 patients had nodal metastasis around the abdominal aorta, without any other form of metastasis. Males accounted for 206 patients and females for 142; the mean patient age was 62.9 years (range, 27–87 years). Every patient was followed up in the outpatient clinic every 1–3 month during the first postoperative year, and every 6–12 months thereafter. Patients underwent physical examination, laboratory tests, chest radiography, abdominal computed tomography, and/or ultrasonography, unless there was a confirmed relapse. The tumour markers carcinoembryonic antigen and carbohydrate antigen 19-9 were also measured until relapse. Recurrence was suspected when a new local or distant metastatic lesion was found on serial images and an increase in tumour marker levels was recognised. When progression of the disease was confirmed by repeated imaging studies, the date of the first suspicious radiologic finding was used as the date of initial disease recurrence. The median follow-up period after surgery was 17.9 (1.3–210) months for the patients overall: 69 patients (19.8%) were alive at the census date (June 2009), 239 (68.7%) died because of pancreatic cancer, and 40 (11.5%) died of other causes. Postresection adjuvant therapy information was available for 327 patients, of whom 19 received chemotherapy and radiotherapy, 134 received chemotherapy only, 2 received radiotherapy only, and 172 did not receive any additional therapy.

Pathological examination

All of the ductal carcinomas were pathologically reexamined and were classified according to the World Health Organisation classification (Klöppel *et al*, 2000), UICC TNM classification (Wittekind *et al*, 2005), and the Classification of Pancreatic Carcinoma of the Japan Pancreas Society (JPS) (Japan Pancreas Society, 2003). Surgically resected specimens were fixed in 10% formalin and cut into serial 5-mm-thick slices, horizontally in the pancreas head, and sagittally in the pancreas body and tail. All the sections were stained with hematoxylin and eosin for pathological examination. The following histopathological variables were evaluated according to the classification of JPS: tumour histological grade, nerve plexus invasion, and lymphatic, venous, and intrapancreatic neural invasion.

Tumour necrosis in PDCs was reported previously (Couvelard *et al*, 2005; Mitsunaga *et al*, 2005), having been defined as 'confluent cell death in invasive areas of primary cancer, visible at an objective lens magnification of ×4' (Mitsunaga *et al*, 2005), which is the same to the definition having been mentioned in breast cancer. Tumour histology often varies among the organs in which tumours develop. We noticed that small areas of necrosis were evident in PDCs, wherein gland formation by cancer cells was ruptured, usually in association with neutrophil infiltration. We refer to this hereafter as micronecrosis, and to the former as massive necrosis. As sometimes it is difficult to differentiate necrotic lesions into either of these two patterns, we combined these two types of lesions solely as 'necrosis'. The definition of histological necrosis is as follows. Necrosis occurs in cancer tissue regardless of its extent, and is usually found in both cancer cells and cancer stroma (Figure 1). When coagulation necrosis is extensively developed (massive necrosis), it corresponds to what was referred to as necrosis previously (Couvelard *et al*, 2005; Mitsunaga *et al*, 2005). Smaller areas of necrosis (micronecrosis) often recognised adjacent to ruptured cancer-forming tubules is almost always accompanied by neutrophil infiltration (Figure 1).

Interobserver reproducibility in identifying histological characteristics

To test the reproducibility of identification of histological characteristics, five independent observers (SS, HT, MY, KY, and TK) were asked to review 51 examples of IDC that were consecutive cases surgically resected between 1997 and 2000. One slide was selected from each of the 51 cases. This slide was one of the slides containing the maximum cut section of the tumour. The complete set of slides from the 51 cases was sent to the five independent observers, all of whom are general surgical pathologists with no specific expertise in the pancreas, and who encounter pancreas specimens rarely. One observer (HT) specialises in breast and female genitourinary pathology and one (SS) in

Table 1 Relationship between clinicopathological characteristics and histological necrosis

Characteristics	No. of patients	Necrosis		P
		Presence	Absence	
Age, years				
<60	123	75	48	
⩾60	225	148	77	0.414
Sex				
Male	206	143	63	
Female	142	80	62	**0.017**
Localisation				
Pancreas head	228	147	81	
Pancreas body or tail	109	70	39	1.000
Size (mm)				
<30	83	42	41	
⩾30	265	181	84	**0.004**
Pathologic tumour status				
T1	6	1	5	
T2	3	3	0	
T3	339	219	120	
T4	0	0	0	**0.023**[a]
Pathologic node status				
N0	64	33	31	
N1	284	190	94	**0.030**
Pathologic metastasis status				
M0	310	193	117	
M1	38	30	8	**0.049**
Stage				
IA	3	0	3	
IB	2	2	0	
IIA	59	31	28	
IIB	246	160	86	
III	0	0	0	
IV	38	30	8	**0.009**[a]
Tumour histological grade[b]				
W/D	90	41	49	
M/D	181	122	59	
P/D	77	60	17	**<0.0001**[a]
Tumour margin status				
Negative	249	166	82	
Positive	100	57	43	0.085
Nerve plexus invasion[b]				
Absence	112	65	47	
Presence	236	158	78	0.120
Lymphatic invasion[b]				
0, 1	102	58	44	
2, 3	246	165	81	0.086
Venous invasion[b]				
0, 1	124	63	61	
2, 3	224	160	64	**0.0002**
Intrapancreatic neural invasion[b]				
0, 1	141	86	55	
2, 3	207	137	70	0.363
Recurrent site[c]				
Local	54	39	15	
Distant sites	198	134	64	0.620
Expression of CAIX in cancer cells[d]				
Absence	114	69	45	
Presence	89	63	26	0.143
Expression of CAIX in stromal cells[d]				
Absence	74	31	43	
Presence	129	101	28	**<0.0001**
Total	348	223	125	

Abbreviations: CAIX = carbonic anhydrase IX; M/D = moderately differentiated adenocarcinoma; P/D = poorly differentaited adenocarcinoma; W/D = well-differentiated adenocarcinoma. [a]Comparisons of qualitative variables are performed using the χ^2 test, and otherwise by Fisher's exact test. [b]Classified according to the classification of pancreatic carcinoma of Japan Pancreas Society. [c]Number of patients with tumour recurrence was 252. [d]Number of patients used in the immunohistochemical analysis was 203. Statistically significant in bold values.

gastrointestinal tract pathology. These observers were provided with the definition of 'histological necrosis' according to Figure 1 and with the definitions for lymphatic, venous, and neural invasion stated in the classification of JPS (Japan Pancreas Society, 2003). They were asked to assess the presence of histological necrosis and each of the grades of lymphatic, venous, and neural invasion evident within each of the provided slides. These observers were blind to the identity of the original reviewers or those of each other. They were also not provided with any clinical information on the outcome of the patients.

Immunohistochemical analysis

Immunohistochemistry was performed on formalin-fixed, paraffin-embedded tissue sections as described previously (Takahashi *et al*, 2007), using antibodies against CAIX (M75, 1:200) (Pastorekova *et al*, 1992; Zavada *et al*, 2000) and HIF-1α (54, 1:500, BD Transduction Laboratories, Franklin Lakes, NJ, USA). Avidin–biotin complex method and CSA system (DAKO, Glostrup, Denmark) were used for these immunohistochemistry, respectively. The sections were autoclaved in the buffer (pH 9.0, Nichirei Biosciences, Tokyo, Japan) for antigen retrieval. For immunohistochemical examination of CAIX in PDCs, we used sections of representative blocks from 203 cases of PDC. Carbonic anhydrase IX is expressed always in the crypt enterocytes of the duodenum and sometimes in normal epithelial cells of the pancreatic duct and pancreatic intraepithelial neoplasm. These cells were used as the positive control for CAIX immunohistochemistry. Immunohistochemistry was performed without primary antibody for negative control. When more than 20% of cancer cells in the specimen expressed CAIX, the case was judged as positive for CAIX in cancer cells. When there were any stromal cells expressing CAIX in cancer tissue, the case was judged as presence of stromal cells expressing CAIX.

Statistical analysis

Comparisons of qualitative variables were performed using the χ^2 test or Fisher's exact test. One-way analysis of variance was used to compare the means of three or more groups. The postoperative disease-free survival (DFS) and disease-specific survival (DSS) rates were calculated by the Kaplan–Meier method. Univariate analysis was performed for prognostic factors using the log-rank test. The factors found to be predictive by univariate analysis were subjected to multivariate analysis using the Cox proportional hazards model (backward elimination method). Interobserver

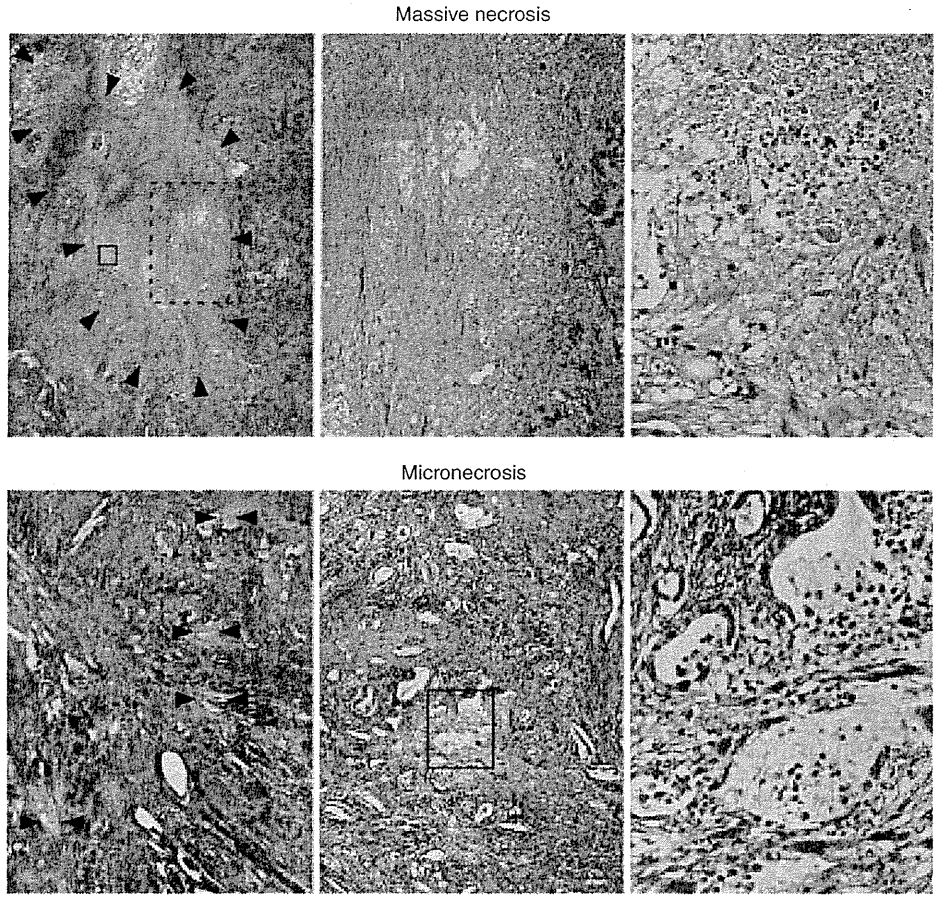

Figure 1 Representative histology of massive necrosis (upper columns) and micronecrosis (lower columns). Arrows indicate necrotic area. Left, centre, and right columns are in low (× 6.25), middle (× 20), and high magnification (× 100), respectively. High power view of histology in right columns corresponds to the rectangle (solid line) in left or middle column. Middle power view of histology in centre columns corresponds to the rectangle (dotted line) in left columns.

agreement (reproducibility) was tested by obtaining the κ-scores (Fleiss, 1971; Landis and Koch, 1977). Differences at $P<0.05$ were considered statistically significant. Statistical analyses were performed with StatView-J 5.0 software (Abacus Concepts, Berkeley, CA, USA).

RESULTS

Correspondence of both massive necrosis and micronecrosis with hypoxic foci

Immunohistochemical analysis revealed that CAIX was expressed in cancer cells or stromal cells within or around areas of both massive necrosis and micronecrosis (Figure 2).

Prognostic significance of the presence of hypoxic foci detected by expression of CAIX in cancer stromal cells

Survival analysis showed that the presence of hypoxic foci with expression of CAIX in stromal cells in cancer tissue was closely associated with shorter DFS ($P=0.004$) and DSS ($P=0.003$) (Figure 3). The presence of cancer cells expressing CAIX was also associated with shorter survival rates (Figure 3), although its occasional expression in cancer cells forming well-differentiated glands distant from necrotic areas probably indicated a cellular phenotype similar to that of normal ductal epithelial cells, and was unrelated to hypoxia. Then we used expression of CAIX in cancer stromal cells as hypoxic marker in this study. Multivariate Cox regression analysis revealed that the presence of hypoxic foci was an independent predictor of shorter DFS ($P=0.005$) and DSS ($P=0.011$) (Supplementary Table 1). The presence of necrosis was significantly correlated with the presence of hypoxic foci (Table 1). More CAIX-expressing cells were found in larger areas of necrosis.

Histopathological evaluation of PDC

Table 1 lists the clinicopathological features of patients with PDC. When correlations with these clinicopathological features were analyzed, the presence of necrosis was found to be more likely in cases with large tumours ($P=0.004$), higher tumour status ($P=0.023$), presence of nodal metastasis ($P=0.030$), presence of distant metastasis ($P=0.049$), higher TNM stage ($P=0.009$), poorer tumour differentiation ($P<0.0001$), and more frequent venous invasion ($P=0.0002$).

Prognostic significance of the histopathological valuables

Survival analysis demonstrated an association between the presence of necrosis and shorter DFS ($P<0.0001$; HR = 2.007; 95% CI: 1.531–2.630) and DSS ($P<0.0001$; HR = 2.196; 95% CI:

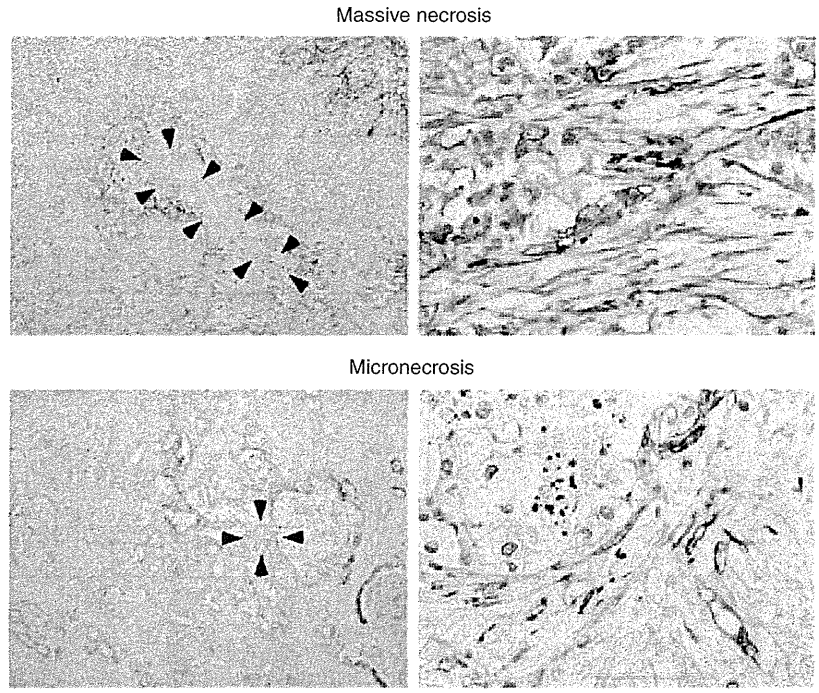

Figure 2 Hypoxia is reflected by the presence of massive necrosis or micronecrosis. Expression of CAIX is immunohistochemically detectable in both cancer cells and stromal cells within or around areas of massive necrosis (upper columns) and micronecrosis (lower columns). Carbonic anhydrase IX is expressed in plasma membrane. Arrows indicate necrotic area. Low power view (left columns) and high power view (right columns).

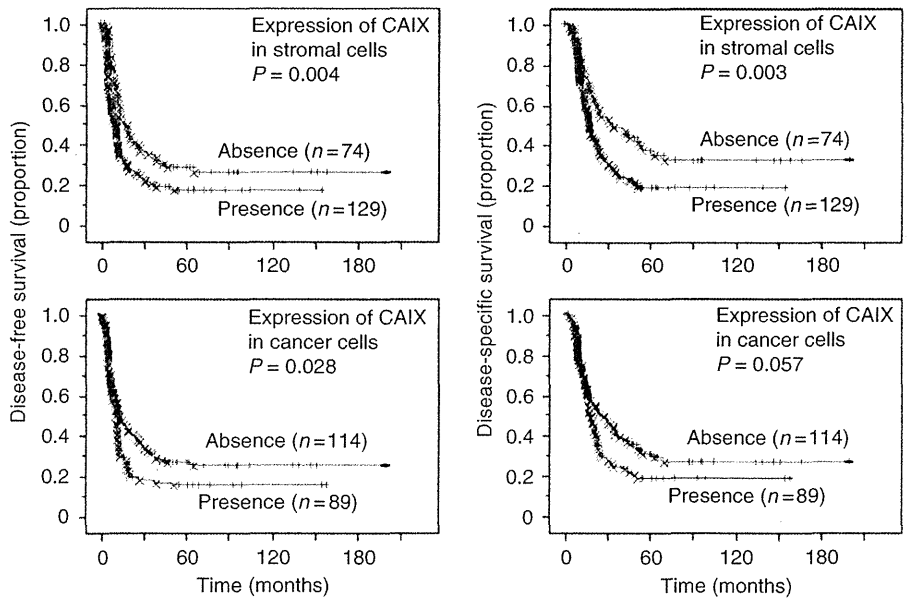

Figure 3 Kaplan–Meier survival curves showing the comparison of disease-free survival between high and low expression of CAIX (*P*-values obtained from log-rank test) (left columns). Kaplan–Meier survival curves showing the comparison of disease-specific survival between high and low expression of CAIX (*P*-values obtained from log-rank test) (right columns).

1.659–2.905) (Figure 4). A similar association was found in patients with PDC at each TNM stages (Figure 4).

The average survival periods for patients having PDC with and without necrosis were 24.62 ± 1.42 months and 47.36 ± 2.75 months, respectively. One-year survival rates for patients having PDC with and without necrosis were 63.3 ± 3.3% and 89.1 ± 2.9%, respectively; the 2-year rates were 36.2 ± 3.4% and 69.0 ± 4.3%, and the 5-year rates were 17.1 ± 2.9% and 40.1 ± 4.8%.

Multivariate Cox regression analysis showed that necrosis ($P<0.0001$; HR = 1.853; 95% CI: 1.407–2.440), metastatic status,